EXTERNAL BIAS EFFECT ON JUNCTION PHOTOLUMINESCENCE IN CdS/CdTe SOLAR CELLS

Diana Shvydka,[1] A.D. Compaan, V.G. Karpov
Department of Physics and Astronomy, University of Toledo, Toledo, OH 43606
[1]Also at First Solar, LLC, 12900 Eckel Junction Rd., Perrysburg, OH 43551

ABSTRACT

We study photoluminescence (PL) from the CdS/CdTe solar-cell junction region. We observed that applied external bias V does not change the spectral shape of the PL signal, but significantly affects the integral PL intensity I(V). It increases with moderate forward bias, tends to saturate when V is above the open-circuit voltage and is suppressed for reverse bias. In the region of forward-bias saturation I(V) is extremely sensitive to device stressing. We attribute the observed phenomena to the field-induced separation of the light-generated electrons and holes. At forward bias above the open circuit voltage, when the field effect is suppressed, PL intensity is dominated by non-radiative recombination.

1. INTRODUCTION

Most photoluminescence (PL) studies in semiconductors have been performed on systems such as single crystals or individual polycrystalline films where the radiative recombination process is affected by defects. Considering photovoltaic devices, one has to take into account that both the carrier excitation and radiative recombination leading to PL may occur in the high electric field induced in the junction region. The CdTe/CdS junction is one such example. The energy gaps of CdTe and CdS are 1.5 eV and 2.5 eV respectively, so that the laser beam of the wavelength 752 nm is absorbed in the ~ 0.3 μm thick CdTe region adjacent to the CdTe/CdS junction, much narrower than the depletion layer width ~ 1-3 μm.

PL intensity is determined by the partial overlap of the electron and hole distributions separated by the field in the junction provided that the non-radiative recombination is relatively inefficient. In the opposite limiting case of weak built-in field, the PL intensity is dominated by the non-radiative recombination before the electrons and holes are spatially separated. By varying the external bias and thus changing the built-in electric field one can observe the crossover between the two regimes and thus characterize the degree of imperfection responsible for non-radiative recombination. From the practical standpoint, observing, under appropriate bias, the crossover between the field- and recombination- dominated PL regimes enables one to detect the presence of defects, which would not show up in the bare built-in field, and thus to characterize the device stability at an earlier stage of its degradation.

2. EXPERIMENTAL

In our experiments [1] we used cells prepared by two different techniques: radio frequency magnetron sputtering and vapor transport deposition. In both cases a layer of CdS followed by a CdTe layer was deposited on commercially available SnO_2-coated glass substrates. The transparent conductive oxide layer served as a front electrode. After deposition, the samples were submitted to a standard anneal in the presence of $CdCl_2$ vapor which generally leads to improved electrical characteristics. Finally, a metal layer was deposited to form the back contact to CdTe.

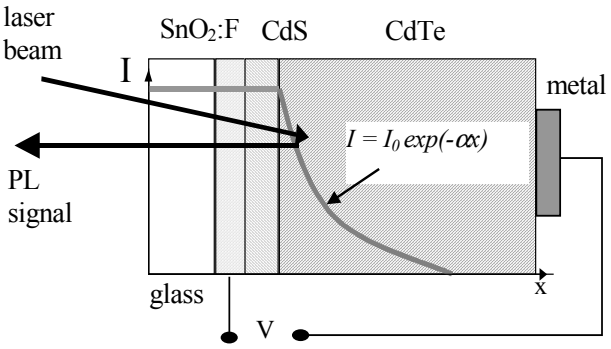

Fig.1 Photoluminescence measurement geometry. Bias voltage is applied between front (SnO_2:F layer) and metal contacts.

The geometry of our photoluminescence measurement is shown in Fig. 1. PL signal was excited with the 752 nm line of a Kr laser focused on the sample with a spot diameter of about 0.5 mm. The luminescence spectrum was collected at room temperature using a triple monochromator and charge coupled device (CCD) detector. Applied external bias did not change the spectrum shape (see Fig. 2); therefore we analyzed the integral PL intensity. Figs. 2-4 show the data for vapor transport deposited solar cells.

The measured bias-dependent PL intensity I(V) shows three distinct features (Figs. 3, 4): (i) rapid increase at $V<V_{oc}$; the open circuit voltage V_{oc} being in the range of

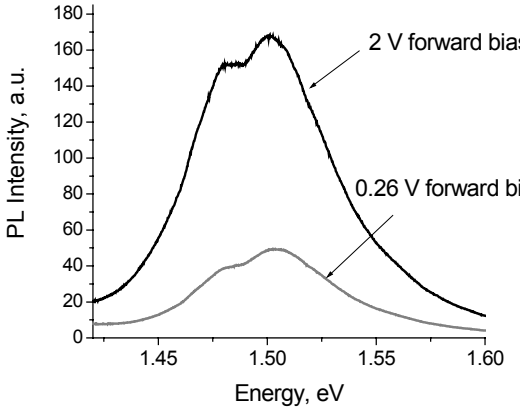

Fig. 2. Photoluminescence spectrum measured under 2 conditions: 0.26 V and 2 V forward bias.

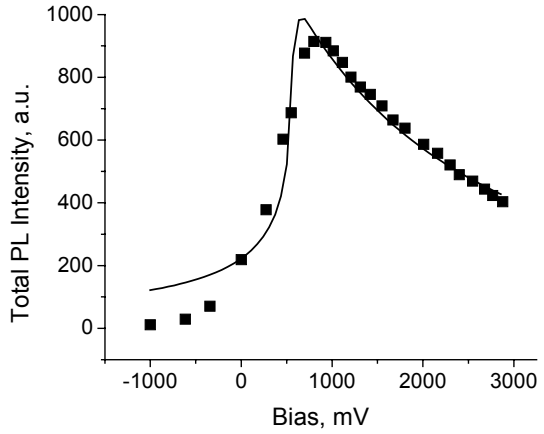

Fig. 3. The measured PL intensity in a wide range of applied biases for an unstressed device. Solid line represents analytical fit by Eq. (2)

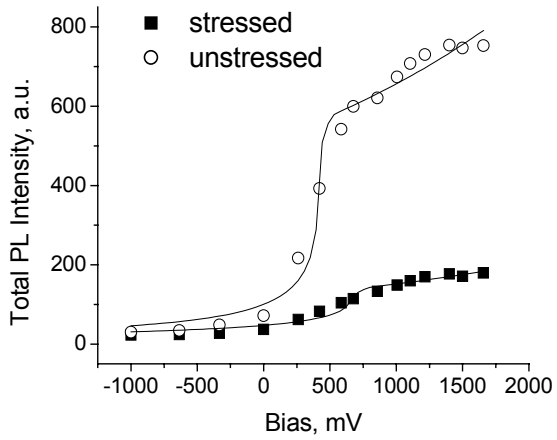

Fig 4. Bias-dependent PL: data (points) under 20-sun laser beam and theoretical fits (curves) by Eq. (2)

700 to 800 mV; (ii) the subsequent saturation, and (iii) gradual decrease in the far forward bias region. While retaining the above qualitative features, the particular I(V) shapes varied considerably between different samples without a significant difference between the vapor transport deposited and sputtered ones. This is illustrated by comparing the data in Fig. 3 and 4, the latter showing a more extended saturation region. A remarkable feature in Fig. 4 is that the saturation region is extremely sensitive to light-soak-induced degradation: a PL signal change by a factor of 5 is observed in response to a 28 days light soak. This is by many orders of magnitude larger than a typical several percent change in the cell efficiency, in accordance with the published data [2].

3. MODEL

Qualitatively our model can be explained as follows (see Fig. 5). The electron-hole pair generation occurs predominantly in a relatively thin CdTe region adjacent to the metallurgical junction. The electrons and holes are swept out by the internal electric field in the junction, which suppresses PL. The reverse bias aggravates this effect by increasing the field in the junction. To the contrary, forward bias creates the opposite electric field and thus promotes PL by moving the electrons and holes towards each other. This explains the general observed trend in PL intensity versus bias.

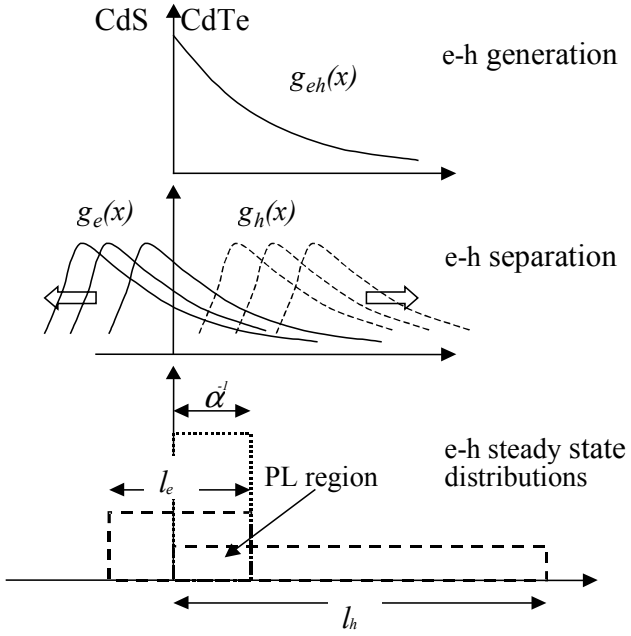

Fig. 5. Field effect on the junction photoluminescence. Here $g_{e(h)}$ is electron (hole) generation, α^{-1} is absorption length and $l_{e(h)}$ is an electron (hole) drift length. For qualitative consideration the electron (hole) distributions are approximated as rectangular.

Superimposed onto the above picture is the nonradiative recombination, which also suppresses PL.

The nonradiative recombination lifetime τ is determined by the defect concentration in the p-n junction region. This time should be compared with τ_d - the time of field-induced drift beyond the junction region. If $\tau > \tau_d$ then the non-radiative recombination is relatively immaterial; this regime may be relevant for the cases of reverse or moderate forward biases. In the opposite case of significant forward bias, the internal electric field is balanced or even reversed and does not make the charged carriers drift fast enough beyond the generation region. Hence, $\tau > \tau_d$ and PL intensity is dominated by the non-radiative recombination. This explains how the observed PL is sensitive to degradation in the significant forward bias region.

4. THEORY

More quantitatively, the physics behind our bias-dependent PL model, explained in the above, can be described by the steady-state balance equation for the space distribution of the light-generated electrons and holes that includes generation (g), drift, and recombination:

$$g(x) - \mu E \frac{\partial n}{\partial x} - \frac{n}{\tau} = 0 \qquad (1)$$

Here μ and E are the mobility and the electric field, n is the electron (hole) concentration, τ is the recombination lifetime, and the origin is at the metallurgical junction: the regions x > 0 and x < 0 correspond to CdTe and CdS respectively. The generation rate contains a step-function of coordinate, $g(x) = g_0 \Theta(x) \exp(-\alpha x)$.

In Eq. (1) we have assumed (i) linear recombination kinetics; (ii) uniform electric field; (iii) negligible role of diffusion, justified for the case of practical interest. The boundary conditions to Eq. (1) are that the electron and hole concentrations remain finite everywhere. Solving Eq. (1) and introducing the electron (hole) drift length, $l_{e(h)} = \mu_{e(h)} E \tau_{e(h)}$ the integral PL intensity becomes

$$I \propto \int n_e n_h dx \propto \frac{g_0^2 \tau_e \tau_h}{\alpha(\alpha l_e + 1)(\alpha l_h + 1)} \qquad (2)$$

Eq. (2) predicts indeed that in the limiting case of strong electric fields, $\alpha l_{e(h)} >> 1$, the PL intensity does not depend on the carrier lifetime and strongly depends on the field. In the opposite limiting case of low electric field, $\alpha l_{e(h)} << 1$, the PL intensity does not depend on the field strength, is proportional to the carrier lifetimes and thus depends on the material degradation. When forward bias is strong enough to reverse the field, the above description can be modified by noting that the field will move the electrons and holes in the directions opposite to those in the above.

To compare the above predictions with the experiment we express E in the terms of external bias V. For the case of reverse or moderate forward bias the depletion region represents the most resistive part of the device and the bias drops there almost entirely. Because the depletion region width is proportional to the square root of the voltage drop, the maximum electric field becomes

$$E(V) = E_0 \sqrt{1 - \frac{V}{V_b}} \text{ for } V < V_b . \qquad (3)$$

The built-in potential V_b is typically close to V_{oc}. As the forward bias balances the built-in field, it distributes more uniformly across the device. This leads to the field-bias dependence that is close to linear,

$$E(V) = E_1 \left(\frac{V}{V_b} - 1 \right) \text{ for } V > V_b . \qquad (4)$$

E_0, E_1, and V_b are considered the device parameters.

5. P-N JUNCTION NUMERICAL MODELING

To verify the predictions of Eqs. (3) and (4) we performed numerical simulations by the AMPS1D software [3] for realistic device parameters shown in Table 1.

Table 1. AMPS: General Layer Parameters (Lifetime Model) [4].

	CdS	CdTe
EPS	9.0	10.0
MUN	350.0 cm^2/V/cm	500.0 cm^2/V/cm
MUP	50.0 cm^2/V/cm	50.0 cm^2/V/cm
NA	1.0 e+014 1/cm^3	1.0 e+015 1/cm^3
ND	1.0 e+015 1/cm^3	0.0 1/cm^3
EG	2.40 eV	1.50 eV
NC	1.8 e+019 1/cm^3	2.8 e+019 1/cm^3
NV	2.4 e+018 1/cm^3	1.04 e+019 1/cm^3
CHI	4.50 eV	4.28 eV
TAU	1.0 e-10 s (holes)	5.0 e-10 s (electrons)

Simulation of the electric field in the junction region is shown in Fig. 6. The CdS/CdTe heterojunction is at x=0.5 with x>0.5 μm being the CdTe region. Table 4.1 shows that the donor density in CdS was assumed the same as the acceptor density in CdTe (p= 5×10^{14} cm^{-3}). It is generally thought that CdS is more heavily doped but since no carriers are collected nor PL received from the CdS the field profile there is not important. The modeling shows that the maximum junction field decreases from about 11 kV/cm at zero bias to ~6 kV/cm at +0.5 V to near zero at V_{OC} and reverses sign, but remains small for forward biases. This behavior corresponds closely to the expected behavior in which carrier sweep-out controls the PL intensity from the junction region.

To fit the data we used the dependence in Eq. (2) with the piece-wise approximation for the electric field in Eqs. (3) and (4). The example in Fig. 7 is consistent with Eqs. (3) and (4). The four fitting parameters $l_0=E_0\mu\tau\alpha$, $l_1=E_1\mu\tau\alpha$ (which are the drift lengths corresponding to the characteristic fields E_0 and E_1, and normalized to the absorption length) , V_b, and $I_0 = g_0^2\tau_e\tau_h\alpha^{-1}$ were set the same for the electrons and holes. Adjusting them independently for each of the two could further improve the fit; however this could hardly be justified given rather approximate character of our model. With that in mind, we find the fit in Figs. 3 and 4 quite satisfactory; the gradual decrease in *I(V)* predicted by the model falls beyond the experimental region in Fig. 4. Typical of our data were V_b slightly smaller than V_{oc}, $I_0 \sim 1$ and $l_1/l_0 \sim 0.1$, consistent with the available data on the CdTe parameters [5]. We also observed that the best-fit parameters I_0, l_0 and l_1 decreased with degradation, such that I_0 scaled approximately as the square of l_0. This observation is consistent with the prediction in Eq. (2) if we assume that the change in the recombination times is the main effect of degradation on the observed PL (the latter changed approximately by the factor of 3 under conditions of this work).

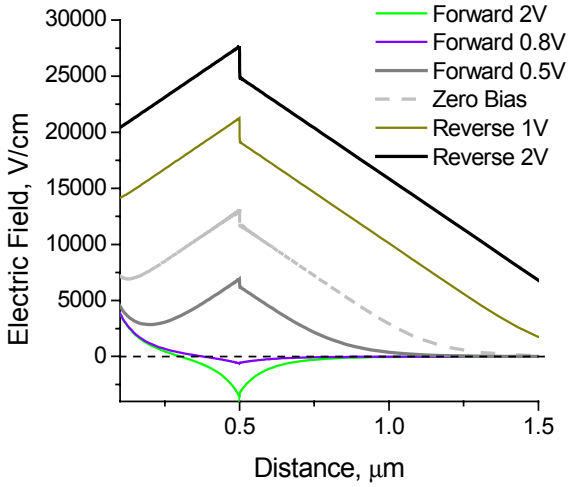

Fig. 6. AMPS-1D generated simulation of the electric field in the junction region.

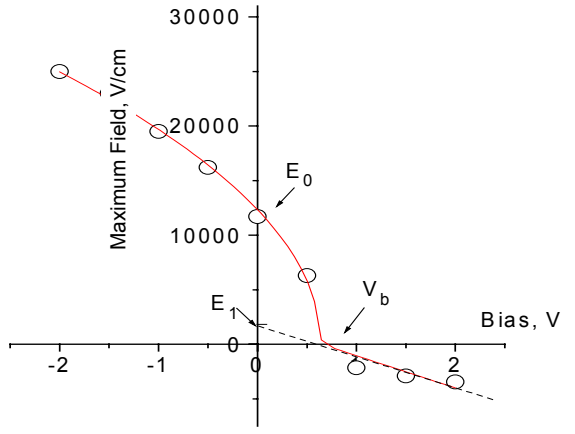

Fig. 7. AMPS-1D simulated data on the field-bias dependence for a CdTe/CdS solar cell (dots) in comparison with the piece-wise approximation in Eqs. (3) and (4) (solid line).

6. CONCLUSIONS

In conclusion, the external bias is shown to significantly affect PL in CdTe photovoltaics. Our data are consistent with the model where PL is suppressed by two competing mechanisms: field induced spatial separation of charge carriers and their non-radiative recombination. We have observed the crossover between the two mechanisms. We have also developed a semi-quantitative model of bias-dependent PL. The main effect of degradation is found to be a decrease in the non-radiative recombination lifetime (possibly by introducing new recombination centers). We emphasize that the defects become visible when the junction field is suppressed by the external bias. This finding can have more general significance: to observe the effects of device degradation at the earliest stage, it may be helpful to balance the junction field. This situation seems also to be approachable by studying electroluminescence where by its setup the built-in field is suppressed. Another ways of achieving similar conditions would be measuring the device characteristics under the circumstances where the charge generation is extremely high, so that the junction field is effectively screened [6].

This work was supported in part by NREL.

REFERENCES

[1] Diana Shvydka, V.G. Karpov , and A.D. Compaan, *Appl. Phys. Lett.* **80**, 2002, p.3114.

[2] S. S. Hegedus, B. E. McCandles, and R. W. Birkmire, *28th IEEE Photovoltaic Specialists Conference Proceedings*, 2000, p.535.

[3] AMPS1D is copyrighted by Penn State University and is available at http://www.psu.edu/dept/AMPS.

[4] See, for example, J.Sites, Annual Report (1994), NREL Subcontract XAX-4-14000-01, p.6 and A.L. Fahrenbruch, NCPV Program Review, AIP Conf. Proc. **462**, 1998, p.48.

[5] A.L. Fahrenbruch, R.H. Bube, *Fundamentals of Solar Cells*, Academic Press, New York, 1983, p.83

[6] R. Harju, V. G. Karpov, D. Grecu, G. Dorer, *J. Appl. Phys.* **88**, 2000, p. 1794.